

a limited  $2\theta$  range between 2.0 and 12.0°.] Systematic absences for  $h0l$  ( $h + l \neq 2n$ ) and  $0k0$  ( $k \neq 2n$ ) were consistent only with space group  $P2_1/n$ . [For 3, the systematic absences  $0kl$  ( $k + l \neq 2n$ ) and  $0hl$  ( $h \neq 2n$ ) were consistent with space groups  $Pna2_1$  and  $Pnam$ . The acentric space group was established from the average values of the normalized structure factors, the successful refinement of the proposed model in the acentric space group, and the orientation of the molecule with respect to the  $c$ -axis.] The measured intensities were reduced to structure factor amplitudes and their esd's by correction for background, scan speed, and Lorentz and polarization effects. While corrections for crystal decay were unnecessary, absorption corrections were applied, the maximum and minimum transmission factors being 0.837 and 0.731. [For 3, the absorption correction was complicated due to the difficulty of indexing the faces. The maximum and minimum transmission factors were 0.867 and 0.826, respectively.] Systematically absent reflections were deleted, and symmetry equivalent reflections were averaged to yield the set of unique data. Only those data with  $I > 2.58\sigma(I)$  were used in the least-squares refinement.

The structure was solved using direct methods (SHELXS-86). The positions of the zirconium and phosphorus atoms were deduced from an E-map [for 3, only the zirconium atoms were located initially]. Subsequent least-squares refinement and difference Fourier syntheses revealed the positions of the remaining atoms. The quantity minimized by the least-squares program was  $\sum w(|F_o| - |F_c|)^2$ , where  $w = 1.21/(\sigma(F_o)^2 + (pF_o)^2)$  [for 3,  $w = 1.04/(\sigma(F_o)^2 + (pF_o)^2)$ ]. The analytical approximations to the scattering factors were used, and all structure factors were corrected for both the real and imaginary components of anomalous dispersion. In the final cycle of least squares, all non-hydrogen atoms were independently refined with anisotropic thermal coefficients, and a group isotropic thermal parameter was varied for the hydrogen atoms. The hydrogen atoms were located in the Fourier difference maps, and their locations were independently refined with isotropic thermal param-

eters. [For 3, anisotropic thermal parameters were refined for the zirconium, phosphorus, and carbon atoms, and isotropic thermal parameters were varied for the boron atoms. Most of the hydrogen atoms appeared in the difference Fourier maps. In the final model, the aliphatic hydrogen atoms were included as fixed contributors in "idealized" positions with C-H = 0.95 Å. In contrast, the positions of hydrogen atoms attached to zirconium and in the BH<sub>4</sub> groups were independently refined. A common isotropic thermal parameter was varied for all the hydrogen atoms.] An isotropic extinction parameter was also refined, which converged to  $2.2(3) \times 10^{-8}$  [for 3,  $3.5(3) \times 10^{-8}$ ]. Successful convergence was indicated by the maximum shift/error of 0.005 [for 3, 0.003] in the last cycle. Final refinement parameters are given in Table II. The final difference Fourier map had no significant features. There were no apparent systematic errors among the final observed and calculated structure factors.

**Acknowledgment.** We thank the Department of Energy (Grant DE-AC02-76ER-01198) for support of this work. We thank Charlotte Stern of the University of Illinois X-ray Crystallographic Laboratory for assisting with the crystal structure determinations and Yujian You for carrying out one NMR study. G.S.G. is the recipient of a Henry and Camille Dreyfus Teacher-Scholar Award (1988-1993).

**Supplementary Material Available:** Tables of atomic coordinates, thermal parameters, and bond distances and angles for Zr<sub>3</sub>H<sub>6</sub>(BH<sub>4</sub>)<sub>6</sub>(PMe<sub>3</sub>)<sub>4</sub> and Zr<sub>2</sub>H<sub>4</sub>(BH<sub>4</sub>)<sub>4</sub>(dmpe)<sub>2</sub> and calculated hydrogen atom positions for Zr<sub>2</sub>H<sub>4</sub>(BH<sub>4</sub>)<sub>4</sub>(dmpe)<sub>2</sub> (15 pages); tables of final observed and calculated structure factors for Zr<sub>3</sub>H<sub>6</sub>(BH<sub>4</sub>)<sub>6</sub>(PMe<sub>3</sub>)<sub>4</sub> and Zr<sub>2</sub>H<sub>4</sub>(BH<sub>4</sub>)<sub>4</sub>(dmpe)<sub>2</sub> (31 pages). Ordering information is given on any current masthead page.

## Efficient Transfer-Dehydrogenation of Alkanes Catalyzed by Rhodium Trimethylphosphine Complexes under Dihydrogen Atmosphere

John A. Maguire, Angelo Petrillo, and Alan S. Goldman\*

Contribution from the Department of Chemistry, Rutgers, The State University of New Jersey, New Brunswick, New Jersey 08903. Received June 17, 1992.  
Revised Manuscript Received July 31, 1992

**Abstract:** RhL<sub>2</sub>Cl(CO) (1; L = PMe<sub>3</sub>), a known catalyst for the photodehydrogenation of alkanes, is found to catalyze the highly efficient thermal (nonphotochemical) transfer-dehydrogenation of alkanes under high-pressure hydrogen atmosphere. The proposed mechanism involves addition of H<sub>2</sub>, loss of CO, and transfer of H<sub>2</sub> to a sacrificial acceptor, thereby generating RhL<sub>2</sub>Cl, the same catalytically active fragment formed by photolysis of 1. Consistent with this proposal, we report that photochemically inactive species, RhL<sub>2</sub>ClL' (L' = PPr<sub>3</sub>, PCy<sub>3</sub>, PMe<sub>3</sub>) and [RhL<sub>2</sub>Cl]<sub>2</sub>, are also thermochemical catalyst precursors. These species demonstrate much greater catalytic activity than RhL<sub>2</sub>Cl(CO), particularly under moderate hydrogen pressures (ca. 500 times greater under 800 Torr of H<sub>2</sub> at 50 °C). The dependence of the turnover rates on hydrogen pressure is consistent with the proposed role of hydrogen, i.e., displacement of L' from the four-coordinate complexes or fragmentation of H<sub>2</sub>RhL<sub>2</sub>Cl<sub>2</sub>, giving H<sub>2</sub>RhL<sub>2</sub>Cl, which is dehydrogenated by olefin to give RhL<sub>2</sub>Cl. Selectivity studies provide further support for the characterization of the active fragment.

The catalytic functionalization of alkanes is currently one of the major challenges of organometallic chemistry.<sup>1,2</sup> Dehydrogenation to give alkenes is one potential functionalization that is attractive in view of the versatility of alkenes as precursors for a wide range of useful and facile transformations. The ability of organometallic complexes to catalyze alkene hydrogenation with remarkable effectiveness<sup>3</sup> is promising in the context of dehydrogenation. Indeed, alkane transfer-dehydrogenation systems (i.e., systems using a sacrificial hydrogen acceptor), first developed

by Crabtree and Felkin, have long stood as the foremost examples of organometallic-catalyzed alkane functionalization.<sup>4,5</sup> However,

(1) For reviews of alkane C-H bond activation by organometallic complexes see: (a) Bergman, R. G. *Science (Washington, D.C.)* **1984**, *223*, 902. (b) Janowicz, A. H.; Periana, R. A.; Buchanan, J. M.; Kovac, C. A.; Stryker, J. M.; Wax, M. J.; Bergman, R. G. *Pure Appl. Chem.* **1984**, *56*, 13-23. (c) Crabtree, R. H. *Chem. Rev.* **1985**, *85*, 245. (d) Halpern, J. *Inorg. Chim. Acta* **1985**, *100*, 41-48. (e) Jones, W. D.; Feher, F. J. *Acc. Chem. Res.* **1989**, *22*, 91 and ref 2.

(2) For a general review of homogeneous alkane functionalization with an emphasis on catalysis see: *Activation and Functionalization of Alkanes*; Hill, C., Ed.; John Wiley & Sons: New York, 1989.

\* To whom correspondence should be addressed at the Department of Chemistry, Rutgers University Piscataway, NJ 08855-0939.

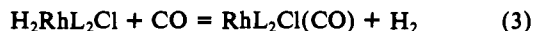
**Table I.** Transfer-Dehydrogenation of Various Saturated Hydrogen Donors and Unsaturated Acceptors Catalyzed by **1** (60 °C; 100-min Reaction Time)<sup>a</sup>

saturated substrate ( $\Delta H^\circ$ (degeneration), kcal/mol) <sup>17</sup>	hydrogen acceptor (concn)	dehydrogenated product (mol/mol of <b>1</b> )	hydrogenated product (mol/mol of <b>1</b> )
cycloheptane (26.3)	norbornene (1.35 M)	cycloheptene (53)	norbornane (230)
cyclohexane (28.2)	norbornene (1.35 M)	cyclohexene (1.7)	norbornane (330)
tetrahydrofuran	norbornene (1.35 M)	2,3-dihydrofuran (106)	norbornane (340)
		2,5-dihydrofuran (18)	
		furan (6)	
<i>n</i> -hexane (27.0–30.0) <sup>b</sup>	norbornene (1.35 M)	hexenes (9.6) <sup>b</sup>	norbornane (250)
cyclooctane (23.3)	norbornene (1.35 M)	cyclooctene (59)	norbornane (360)
cyclooctane	cyclohexene (1.58 M)	cyclooctene (106)	cyclohexane (360)
cyclooctane	cycloheptene (1.35 M)	cyclooctene (53)	cycloheptane (1400)
cyclooctane	<i>tert</i> -butylethylene (1.24 M)	cyclooctene (4)	<i>tert</i> -butylethane (60)
cyclooctane	ethylene (200 psi)	cyclooctene (12)	ethane

<sup>a</sup> Conditions: [1] = 0.4 mM;  $P_{H_2}$  = 1000 psi; 60 °C. All products and concentrations determined by gas chromatography in comparison with authentic (commercial) samples. The identity of the cyclooctene and norbornane products from a run with cyclooctane substrate and norbornene acceptor was confirmed by GC/MS. <sup>b</sup> Mixture of hexenes.

even those systems do not yield high catalytic turnover numbers (>70).

Several years ago, it was discovered that  $RhL_2Cl(CO)$  **1**;  $L = PMe_3$  catalyzes the photodehydrogenation of alkanes with high chemical and quantum efficiencies.<sup>6–8</sup> Our mechanistic study of this reaction<sup>8,9</sup> revealed two key points: (1) The fragment  $RhL_2Cl$ , generated by photochemical CO extrusion<sup>10</sup> (eq 1), reacts *thermally* with alkanes (via oxidative addition and  $\beta$ -hydrogen elimination) to give alkene and  $H_2RhL_2Cl$  (eq 2). (2) Subsequently,  $H_2RhL_2Cl$  reacts with CO to regenerate **1** (eq 3).



It is noteworthy that two characteristic properties of the CO ligand, high photolability and facile formation of strongly bound complexes, favor reactions 1 and 3, respectively. Accordingly, no  $RhL_2ClL'$  complex other than **1** ( $L' = CO$ ) has been found to efficiently catalyze photodehydrogenation.

In this paper, we report that the catalytically active fragment  $RhL_2Cl$ <sup>11–14</sup> can be accessed thermally (nonphotochemically) via

(3) Collman, J. P.; Hegedus, L. S.; Norton, J. R.; Finke, R. C. *Principles and Applications of Organotransition Metal Chemistry*; University Science Books: Mill Valley, CA, 1987; pp 523–548.

(4) (a) Burks, M. J.; Crabtree, R. H.; Parnell, C. P.; Uriarte, R. J. *Organometallics* **1984**, *3*, 816–817. (b) Burk, M. J.; Crabtree, R. H.; McGrath, D. V. *J. Chem. Soc., Chem. Commun.* **1985**, 1829–1830. (c) Burk, M. J.; Crabtree, R. H. *J. Am. Chem. Soc.* **1987**, *109*, 8025–8032.

(5) (a) Baudry, D.; Ephritikine, M.; Felkin, H.; Holmes-Smith, R. J. *J. Chem. Soc., Chem. Commun.* **1983**, 788–789. (b) Felkin, H.; Fillebeen-Khan, T.; Gault, Y.; Holmes-Smith, R.; Zakrzewski, J. *Tetrahedron Lett.* **1984**, *26*, 1999–2000. (c) Felkin, H.; Fillebeen-Khan, T.; Holmes-Smith, R.; Lin, Y. *Tetrahedron Lett.* **1985**, *26*, 1999–2000.

(6) Nomura, K.; Saito, Y. *J. Chem. Soc., Chem. Commun.* **1988**, 161.

(7) (a) Sakakura, T.; Sodeyama, T.; Tokunaga, M.; Tanaka, M. *Chem. Lett.* **1988**, 263–264. (b) Sakakura, T.; Sodeyama, T.; Tanaka, M. *Chem. Ind. (London)* **1988**, 530–531. (c) Sakakura, T.; Sodeyama, T.; Tanaka, M. *New J. Chem.* **1989**, *13*, 737–745. (d) Tanaka, M.; Sakakura, T. *Pure Appl. Chem.* **1990**, *62*, 1147–1150. (e) Sakakura, T.; Sodeyama, T.; Abe, F.; Tanaka, M. *Chem. Lett.* **1991**, 297–298.

(8) Maguire, J. A.; Boese, W. T.; Goldman, A. S. *J. Am. Chem. Soc.* **1989**, *111*, 7088–7093.

(9) Maguire, J. A.; Boese, W. T.; Goldman, M. E.; Goldman, A. S. *Coord. Chem. Rev.* **1990**, *97*, 179–192.

(10) Spillet, C. T.; Ford, P. C. *J. Am. Chem. Soc.* **1989**, *111*, 1932–1933.

(11) Isolable bulkier derivatives of  $RhL_2Cl$  are well-known (see refs 12–14). In the case of  $Rh(PCy_3)_2Cl$ , dehydrogenation of the ligand occurs to give  $H_2Rh(PCy_3)_2Cl$  and  $Rh(PCy_3)(\eta^2-PCy_2[C_6H_9])Cl$ .<sup>12</sup>

(12) Heitkamp, S.; Stufkens, D. J.; Vrieze, K. *J. Organomet. Chem.* **1978**, *152*, 347–357.

(13) (a) Van Gaal, H. L. M.; Moers, F. G.; Steggerada, J. J. *J. Organomet. Chem.* **1974**, *65*, C43–C45. (b) Van Gaal, H. L. M.; Van Den Bekerom, F. L. A. *J. Organomet. Chem.* **1977**, *134*, 237–248.

(14) James, B. R.; Preece, M.; Robinson, S. R. In *Catalytic Aspects of Metal Phosphine Complexes*; Alyea, E. C., Meek, D. W., Eds.; *Advances in Chemistry Series 196*; American Chemical Society: Washington, DC, 1982; pp 145–161.

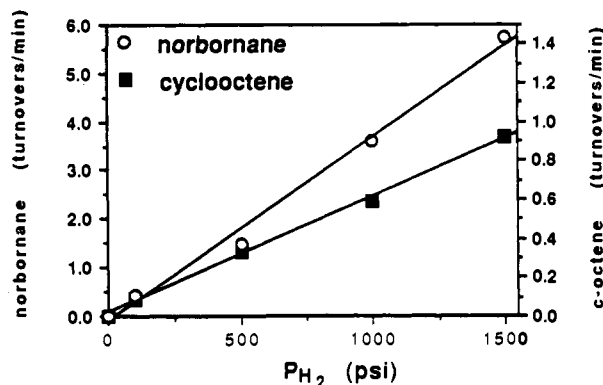
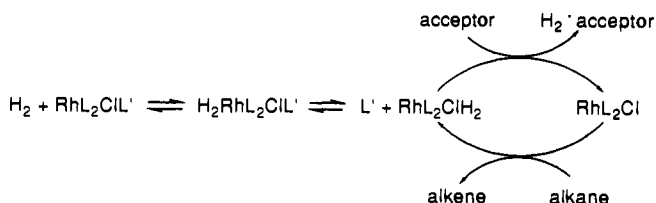


**Figure 1.** Rate versus hydrogen pressure for cyclooctane–norbornene transfer-dehydrogenation catalyzed by **1**. Reaction conditions: cyclooctane solvent; [1]<sub>0</sub> = 0.4 mM; 60 °C; [norbornene]<sub>0</sub> = 1.35 M.

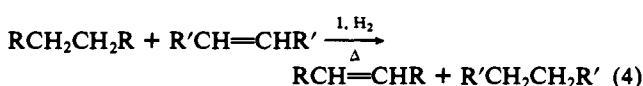
#### Scheme I



the microscopic reverse of eqs 3 and 2, i.e., from **1** in the presence of alkenes and hydrogen atmosphere. As a result, transfer-dehydrogenation of alkanes is catalyzed with remarkably high efficiency.<sup>15</sup> Even greater activity, with the use of much lower hydrogen pressures, is obtained using other (photoinactive) complexes containing the  $RhL_2Cl$  fragment, e.g.,  $RhL_2Cl(P^iPr_3)$  and  $[RhL_2Cl]_2$ .

#### Results and Discussion

**Thermal Transfer-Dehydrogenation Catalyzed by 1.** We recently communicated that **1** catalyzes the highly efficient, thermal (nonphotochemical) transfer-dehydrogenation of alkanes in the presence of olefinic hydrogen acceptors *under high hydrogen pressure*.<sup>15</sup>



This is the first efficient organometallic-based system for thermal catalytic alkane functionalization;<sup>2</sup> for example, at 100 °C, a cyclooctane solution of **1** (0.40 mM) and norbornene (3.8 M)

(15) Maguire, J. A.; Goldman, A. S. *J. Am. Chem. Soc.* **1991**, *113*, 6706–6708.

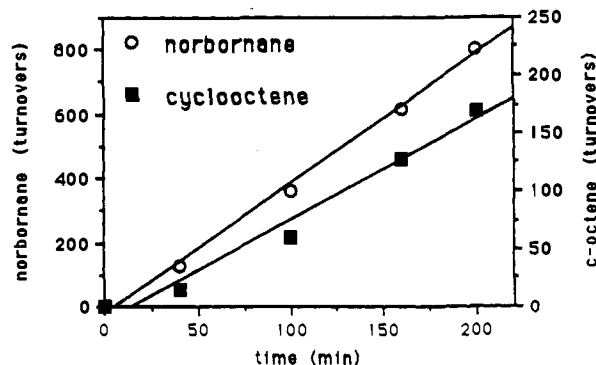


**Figure 2.** Formation of products versus time for cyclooctane-norbornene transfer-dehydrogenation catalyzed by **1**. Reaction conditions: cyclooctane solvent;  $[1]_0 = 0.4$  mM;  $60$  °C;  $[\text{norbornene}]_0 = 1.35$  M;  $P_{\text{H}_2} = 1000$  psi.

under 1000 psi of  $\text{H}_2$  yields 950 turnovers of cyclooctene (0.19 M) in under 15 min.

Even the very high turnover numbers obtained are not limited by catalyst decomposition but rather by complete hydrogenation of the alkene hydrogen acceptor. IR spectroscopy of reaction solutions after several hundred turnovers reveals no diminution of the characteristic C–O stretch of **1** ( $1956\text{ cm}^{-1}$ ). UV–visible observation of the solutions during (under 1000 psi of  $\text{H}_2$ ) and after catalysis shows no change in the spectrum. There is no visible loss of clarity and the reaction is unaffected by the addition of mercury to the reaction mixture, implying that the active catalytic species is not colloidal.<sup>16</sup>

Experimental data obtained with a variety of alkanes and acceptors at  $60$  °C are given in Table I. Cyclooctane, which has an anomalously low enthalpy of dehydrogenation ( $23.3\text{ kcal/mol}^{17}$ ), is a particularly reactive substrate. Note however that comparably high turnover numbers for cycloheptane dehydrogenation ( $26.3\text{ kcal/mol}^{17,18}$ ) can also be obtained (Table I). The reaction rate is independent of norbornene (acceptor) concentration above ca.  $0.3$  M. The nature of the alkene acceptor seems much less critical than with previously reported transfer-dehydrogenation systems;<sup>4,5</sup> a wide variety of olefins including ethylene is suitable (Table I).

Figure 1 reveals a linear dependence of the dehydrogenation rate on hydrogen pressure. Our explanation for the observed catalytic activity, and particularly the unusual hydrogen dependence, is indicated in Scheme I and is based on the photocatalytic mechanism of eqs 1–3. Thus, entry into the cycle of Scheme I is the microscopic reverse of eq 1 (where  $L' = \text{CO}$ ). The cycle itself is composed of the reverse of eq 2 (where the alkene plays the role of the sacrificial acceptor) and then the forward reaction, eq 2. The presumed intermediate,  $\text{H}_2\text{RhL}_2\text{Cl}(\text{CO})$ , is not observable even under 1500 psi of  $\text{H}_2$  in a cell which permits UV-visible spectroscopic monitoring; thus, the preequilibria of Scheme I ( $L' = \text{CO}$ ) lie far to the left. Accordingly, reaction 4 is completely suppressed by even low pressures of added carbon monoxide (5 Torr; ca.  $5 \times 10^{-5}$  M<sup>19</sup>). Monitoring the progress of the reaction at various time intervals reveals that within the limits of experimental error a constant reaction rate is reached within 40 min at  $60$  °C (Figure 2). An apparently lower initial rate may be attributable to the time necessary for the system to reach

**Table II.** Transfer-Dehydrogenation of Cyclooctane Catalyzed by Various Complexes Containing the Fragment  $\text{RhL}_2\text{Cl}$  ( $50$  °C)<sup>a</sup>

catalyst precursor	$P_{\text{H}_2}$ , atm	turnovers, (mol/mol of Rh)/h		
		dehydrogenation	hydrogenation	dehydrogenation:hydrogenation
$\text{RhL}_2\text{Cl}(\text{CO})^{b-d}$	1.05	0.04	0.3	0.13
$\text{RhL}_2\text{Cl}(\text{CO})^{b-d}$	40	1.5	12	0.13
$\text{Rh}(\text{P}^i\text{Pr}_3)_2\text{Cl}(\text{CO})^{b,e}$	40	<0.1	54	<0.002
$\text{RhL}_2\text{Cl}(\text{P}^i\text{Pr}_3)^e$	0.13	27	160	0.17
$\text{RhL}_2\text{Cl}(\text{P}^i\text{Pr}_3)^e$	1.05	44	240	0.18
$\text{RhL}_2\text{Cl}(\text{P}^i\text{Pr}_3)^e$	3.0	42	330	0.13
$\text{RhL}_2\text{Cl}(\text{P}^i\text{Pr}_3)^e$	37	60	1100	0.054
$\text{RhL}_2\text{Cl}(\text{P}^i\text{Pr}_3)^b$	1.05	19	152	0.13
$\text{RhL}_2\text{Cl}(\text{P}^i\text{Pr}_3)/\text{DBU}$ (3 mM) <sup>b</sup>	1.05	23	148	0.16
$\text{RhL}_3\text{Cl}^b$	1.05	3.4	16	0.21
$[\text{RhL}_2\text{Cl}]_2^e$	0.13	20	79	0.25
$[\text{RhL}_2\text{Cl}]_2^e$	40	274	1850	0.15

<sup>a</sup> Turnover numbers determined by gas chromatography. Conditions unless indicated otherwise:  $50$  °C, cyclooctane solution;  $1.0$  mM catalyst. See footnote a, Table I.<sup>37</sup> <sup>b</sup>  $2.0$  M cyclohexene acceptor. <sup>c</sup>  $2.0$  M catalyst. <sup>d</sup> Turnover rates extrapolated from experiments with varied temperature ( $50$ – $100$  °C;  $100$  atm of  $\text{H}_2$ ) and  $\text{H}_2$  pressure ( $7$ – $100$  atm;  $60$  °C). <sup>e</sup>  $1.7$  M norbornene acceptor.

an equilibrium in which CO is partitioned between ligand, solution, and atmospheric CO. Consistent with such an equilibrium, the rate decreases with an increasing ratio of solution- to gas-phase volume.<sup>20</sup> Varying the stirring rate does not affect the reaction rate, indicating that this reflects an equilibrium, not a diffusion-limited process (see Experimental Section). Using different grades of hydrogen also does not affect the rate, arguing against the possibility that impurities in the hydrogen are important. Added  $\text{PMe}_3$  ( $0.4$  mM) completely suppresses reaction 4; conceivably, this may simply be due to CO formed along with small quantities of  $\text{RhL}_3\text{Cl}$ .

The formation of  $\text{RhL}_2\text{Cl}$ , as indicated in Scheme I, is effected by coupling CO loss with alkene hydrogenation. Although metal–carbonyl bond strengths are not well-known for square planar complexes, BDE's for second-row transition metal complexes are generally under  $40\text{ kcal/mol}^{21}$ . If this is the case for **1**, then the CO-loss/alkene-hydrogenation couple, with the alkene acceptors used, is endothermic by less than  $12\text{ kcal/mol}^{18}$ .

As noted above, the high photolability of CO and the facile formation of strongly bound complexes favor the photocatalysis of eqs 1–3. Regarding the mechanism of Scheme I however, photolability is irrelevant and strong binding should *disfavor* catalytic activity. We therefore investigated (photoinactive)  $\text{RhL}_2\text{ClL}'$  complexes, where  $L'$  is more weakly bound than CO.

**$\text{RhL}_2\text{ClL}'$  ( $L' = \text{Phosphine}$ ).** The preequilibria of Scheme I should be favored by a ligand  $L'$ , which is sterically bulky, thus favoring Rh– $L'$  bond disruption. Phosphines were investigated since they offer the opportunity to “fine-tune” steric factors, and the corresponding, easily synthesized, complexes are well-known to add dihydrogen.<sup>3</sup> Accordingly, in support of Scheme I,  $\text{RhL}_2\text{Cl}(\text{P}^i\text{Pr}_3)$  is found to effect rapid transfer-dehydrogenation of alkanes in the presence of hydrogen-acceptors under low  $\text{H}_2$  pressures (Table II), e.g., affording up to 640 turnovers of cyclooctane in 18 h at  $50$  °C ( $1.0$  mM  $\text{RhL}_2\text{Cl}(\text{P}^i\text{Pr}_3)$ ; 800 Torr of  $\text{H}_2$ ;  $2.0$  M norbornene acceptor). Under the same conditions **1** is only ca.  $1/500$  as reactive as  $\text{RhL}_2\text{Cl}(\text{P}^i\text{Pr}_3)$  (Table II). As is observed for **1**, in the absence of  $\text{H}_2$ , no transfer-dehydrogenation is catalyzed ( $<0.02$  turnover/h at  $50$  °C). The catalytic activity reported here is orders of magnitude greater than that of earlier transfer-dehydrogenation systems, e.g., 70 turnovers in 30 days at  $150$  °C.<sup>5</sup>

<sup>1</sup>H NMR spectroscopy of a  $\text{RhL}_2(\text{P}^i\text{Pr}_3)\text{Cl}$  solution under  $\text{H}_2$  atmosphere reveals that *cis,trans*- $\text{H}_2\text{RhL}_2(\text{P}^i\text{Pr}_3)\text{Cl}$ , the proposed

(16) Anton, D. R.; Crabtree, R. H. *Organometallics* 1983, 2, 855–859.

(17) Stull, D. R.; Westrum, E. F.; Sinke, G. C. *The Chemical Thermodynamics of Organic Compounds*; Robert E. Krieger Publishing: Malabar, FL, 1987.

(18) Enthalpies of alkane dehydrogenation range from that of cyclooctane ( $23.3\text{ kcal/mol}$ ) to that of *tert*-butylethane ( $34.0\text{ kcal/mol}$ ). For typical examples, the formation of alkanes from *n*-butane, the following enthalpies (kcal/mol) can be calculated: *trans*-2-butene, 27.5; *cis*-2-butene, 28.5; 1-butene, 30.1.

(19) The solubility of CO in alkanes is estimated to be approximately equal to that in benzene; under 800 Torr  $[\text{CO}] = 0.0072$  M: Linke, W. F. *Solubilities of Inorganic and Metal Organic Compounds*, 4th ed.; D. Van Nostrand Co.: Princeton, NJ, 1958; Vol. 1, p 453.

(20) In one experiment, a  $1.0$ -mL sample of a cyclooctane solution of **1** ( $0.4$  mM) and norbornene ( $1.7$  M) under 1000 psi of  $\text{H}_2$  at  $60$  °C gave 59.9 turnovers of cyclooctane after 100 min. A  $7.0$ -mL sample of the same solution under identical conditions gave only 7.6 turnovers of cyclooctane.

(21) See ref 15, refs 10–16 therein.

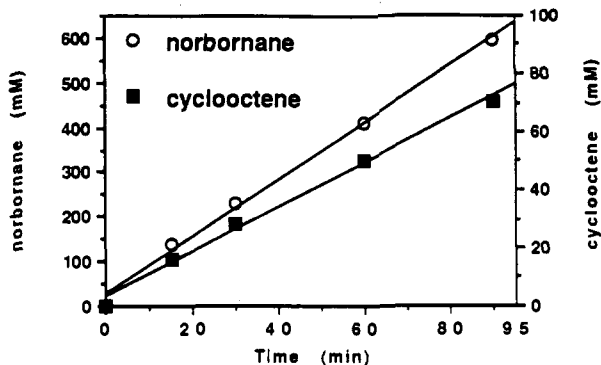


**Figure 3.** Formation of products versus time for cyclooctane-norbornene transfer-dehydrogenation catalyzed by  $[\text{RhL}_2\text{Cl}]_2$ . Conditions: 50 °C; cyclooctane/benzene solution (5:3); 4.0 mM  $[\text{RhL}_2\text{Cl}]_2$ ; 1.7 M norbornene.

intermediate of Scheme I ( $L' = \text{P}^i\text{Pr}_3$ ), accounts for 62% of the mixture. Also observable (under 800 Torr of  $\text{H}_2$ ) are  $\text{H}_2\text{Rh}(\text{P}^i\text{Pr}_3)_2\text{Cl}$ <sup>12,13,22</sup> (16%) and  $\text{H}_2\text{RhL}_3\text{Cl}$  (22%). UV-visible spectroscopy shows that saturation in  $\text{H}_2$  is reached at or below 100 Torr in the absence of olefin.<sup>23</sup> Under typical reaction conditions however, e.g., in the presence of 1.7 M norbornene, the system is only saturated in  $\text{H}_2$  above ca. 800 Torr. A steady state is apparently reached in the presence of alkene, involving alkene hydrogenation, cyclooctane dehydrogenation, and  $\text{H}_2$  addition to rhodium. Consistent with this behavior and with Scheme I, the rate of dehydrogenation (and also hydrogenation) increases with  $\text{H}_2$  pressure, leveling off at ca. 800 Torr.<sup>23</sup>

$\text{RhL}_2\text{Cl}(\text{PCy}_3)$  ( $\text{Cy} = \text{c-C}_6\text{H}_{11}$ )<sup>13</sup> shows reactivity comparable to that of the  $\text{P}^i\text{Pr}_3$  analogue (see Experimental Section).  $\text{RhL}_3\text{Cl}$ <sup>24</sup> affords turnover rates which are ca. 10% of those of the bulkier complexes (see Table II), in accord with the proposed mechanism which involves loss of one ligand. Phosphines bulkier than  $\text{P}^i\text{Pr}_3$  ( $\text{P}^t\text{Bu}_3$ ,  $\text{P}(\text{o-C}_6\text{H}_4\text{Me})_3$ ) did not react with  $[\text{RhL}_2\text{Cl}]_2$  to form the tris(phosphine) complexes, and their presence had no effect on the catalytic activity of  $[\text{RhL}_2\text{Cl}]_2$  (vide infra). Surprisingly, it was found that  $\text{RhL}_2\text{Cl}(\text{P}(\text{O}^i\text{Pr})_3)$  does not add  $\text{H}_2$  (1600 Torr;  $^1\text{H}$  NMR) and that it does not catalyze dehydrogenation.

We consider a possible role of the added hydrogen as an alternative to that proposed in Scheme I:  $\text{H}_2$  addition and subsequent  $\text{HCl}$  reductive elimination would give hydrides which might be more reactive than the parent chloride. However, the presence of sterically hindered "noncoordinating" bases, which should promote  $\text{HCl}$  elimination, failed to increase catalytic activity. The presence of 2,6-di-*tert*-butylpyridine (DBP) (3 mM) in a solution of  $\text{RhL}_2\text{Cl}(\text{P}^i\text{Pr}_3)$  (1.0 mM) and cyclohexene (2.0 M) under 800 Torr of  $\text{H}_2$  completely suppressed catalysis, although the  $^1\text{H}$  NMR spectrum of such a solution (without olefin) revealed that the consumption of the major species in solution was unaffected by DBP. Possibly, an intermediate such as  $\text{H}_2\text{RhP}_2\text{Cl}$  is deprotonated by DBP, rendering it inactive. A different base, 1,8-diazabicyclo[5.4.0]undec-7-ene (DBU; 3 mM), did not significantly affect the rate of transfer-dehydrogenation (Table II). (DBU·HCl does not react with  $\text{RhL}_2(\text{P}^i\text{Pr}_3)\text{Cl}$ , indicating that DBU is a stronger base than  $\text{RhL}_2(\text{P}^i\text{Pr}_3)\text{Cl}$  and therefore any equilibrium involving loss of  $\text{HCl}$  would indeed be shifted by the presence of DBU.) Addition of mercury to the solution (0.25 mL/mL of solution)

(22) Under these conditions,  $\text{H}_2\text{Rh}(\text{P}^i\text{Pr}_3)_2\text{Cl}$  does not measurably catalyze transfer-dehydrogenation (nor does it do so in the absence of hydrogen atmosphere).  $\text{H}_2\text{Rh}(\text{PMe}_3)_3\text{Cl}$  does catalyze transfer-dehydrogenation, but at rates much slower than observed for solutions of (predominantly)  $\text{H}_2\text{Rh}(\text{PMe}_3)_2(\text{P}^i\text{Pr}_3)\text{Cl}$  (see Table II).

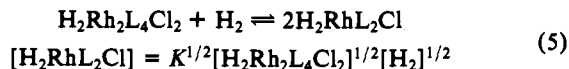
(23) Numerous control experiments were conducted to determine if reaction rates (for kinetic data) or UV-visible spectra were in any way limited by the rate of diffusion of  $\text{H}_2$  into solution. Conditions were chosen such that rates of  $\text{RhL}_2\text{Cl}(\text{P}^i\text{Pr}_3)$ - and  $[\text{RhL}_2\text{Cl}]_2$ -catalyzed runs and spectra were unaffected by varying stirring rate and sample volume.

(24) Jones, R. A.; Real, F. M.; Wilkinson, G.; Galas, A. M.; Hursthouse, M. B.; Malik, K. M. A. *J. Chem. Soc., Dalton Trans.* 1980, 511–518.

also shows no effect, implying that the active species is not colloidal.<sup>16</sup>

$[\text{RhL}_2\text{Cl}]_2$ . The isolable dimer of the proposed active fragment,  $[\text{RhL}_2\text{Cl}]_2$ ,<sup>25</sup> is also an effective transfer-dehydrogenation catalyst (see Figure 3). Under  $\text{H}_2$  atmosphere and in the presence of olefin (e.g., 0.021 M cyclohexene), two rhodium-containing species can be observed by  $^1\text{H}$  NMR: (1)  $\text{H}_2\text{L}_2\text{Rh}(\mu\text{-Cl})_2\text{RhL}_2$ , analogous to the  $\text{P}(\text{p-C}_6\text{H}_4\text{Me})_3$  dimer observed by Tolman,<sup>26</sup> and (2) a complex containing both a bridging and a terminal hydride, likely an isomer of the first species. In the absence of olefin, the same two complexes initially form upon addition of  $\text{H}_2$  to a solution of  $[\text{RhL}_2\text{Cl}]_2$  (thus the complexes obviously do not contain olefin) but, interestingly, they undergo rapid decomposition to give at least five uncharacterized hydride-containing products not observed in the presence of olefin.

The rate of  $[\text{RhL}_2\text{Cl}]_2$ -catalyzed cyclooctane dehydrogenation exhibits a half-order dependence of  $\text{H}_2$  pressure (100 Torr–40 atm;<sup>23</sup>  $[\text{RhL}_2\text{Cl}]_2 = 1.0$  mM;  $[\text{norbornene}]_0 = 1.7$  M) (Figure 4; a plot of  $\log(\text{rate})$  vs  $\log P_{\text{H}_2}$  yields a slope of 0.48). The dependence on the concentration of  $[\text{RhL}_2\text{Cl}]_2$  is also half-order (0.25–4.0 mM; 1600 Torr  $\text{H}_2$ ;  $[\text{norbornene}]_0 = 1.7$  M) (Figure 5; a plot of  $\log(\text{rate})$  vs  $\log [[\text{RhL}_2\text{Cl}]_2]$  yields a slope of 0.53), which is supportive of a mononuclear transition state. More specifically, these results can be rationalized in terms of the equilibrium of eq 5 if the rate of transfer-dehydrogenation is assumed to be proportional to the concentration of  $\text{H}_2\text{RhL}_2\text{Cl}$ , which is consistent with Scheme I.



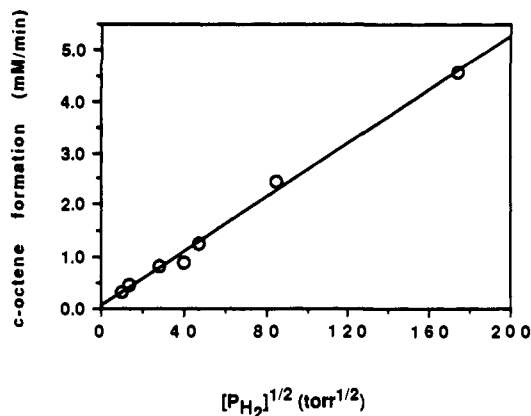
However, the observed dependence on  $[\text{norbornene}]$  is zero order rather than first order as would be expected if the reaction of  $\text{H}_2\text{RhL}_2\text{Cl}$  with alkene were rate-determining (0.17–1.7 M norbornene;  $[[\text{RhL}_2\text{Cl}]_2]_0 = 2.0$  mM;  $P_{\text{H}_2} = 1600$  Torr; 50 °C). Similarly, saturation in  $[\text{norbornene}]$  is observed at concentrations greater than ca. 0.3 M for the 1-based system, as noted above. Although the observed saturation or zero-order dependence may be due to selective solvation by the olefin, we believe it is more likely to result from any of numerous possible side reactions (e.g., addition of olefin to  $\text{RhL}_2\text{Cl}$ ) not included in Scheme I. We tentatively presume that Scheme I, though essentially valid, is an oversimplification of a highly complex system. We note for example the mechanistic complexity of the closely related Wilkinson's catalyst hydrogenation system.<sup>27</sup> A more detailed mechanistic picture of the present systems will require a thorough kinetic study, which is currently underway using what appears to be the simplest of the systems described herein, that based on  $\text{RhL}_3\text{Cl}$ . Unlike the  $[\text{RhL}_2\text{Cl}]_2$ - and  $\text{RhL}_2\text{Cl}L'$ -based systems ( $L' =$  bulky phosphine),  $\text{RhL}_3\text{Cl}$  exists as only one major species under the reaction conditions,  $\text{H}_2\text{RhL}_3\text{Cl}$  (as determined by  $^1\text{H}$  NMR). Further, the system allows the presence of excess  $L'$  ( $L$ ) without changing the ratios of the major components. Selectivity experiments described below support the view of the  $\text{RhL}_3\text{Cl}$  system as the simplest and therefore the most amenable to a thorough mechanistic investigation.

**Selectivity: Comparison of the Photochemical and Thermal Systems.** Intramolecular selectivity studies have been conducted with isopropylcyclohexane as the substrate. The  $\text{RhL}_3\text{Cl}/\text{H}_2$  thermal system and the  $\text{RhL}_2\text{Cl}(\text{CO})$  photochemical system afford distribution of double-bond isomers (Figure 6) which agree within experimental error (ca.  $\pm 20\%$ ) in the limit of short reaction times (the distribution changes with time due to isomerization and/or hydrogenation of products; note that only three of the five possible isomers are detected). This result is consistent with a common active intermediate, presumably  $\text{RhL}_2\text{Cl}$ , the greatest common denominator of the two complexes.<sup>28</sup> Although the same three

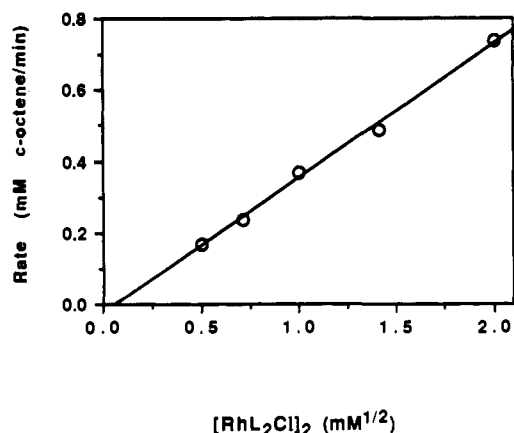
(25) Werner, H.; Feser, R. Z. *Naturforsch.* 1980, 35B, 689–693.

(26) Tolman, C. A.; Meakin, P. Z.; Lindner, D. L.; Jesson, J. P. *J. Am. Chem. Soc.* 1974, 96, 2762–2774.

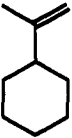
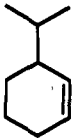
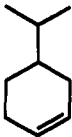
(27) Halpern, J. *Inorg. Chim. Acta* 1981, 50, 11–19.



**Figure 4.** Cyclooctane–norbornene transfer-dehydrogenation catalyzed by  $[RhL_2Cl]_2$  at various hydrogen pressures. Conditions: 50 °C; cyclooctane/benzene solution (4:1); 1.0 mM  $[RhL_2Cl]_2$ ; 1.7 M norbornene.



**Figure 5.** Cyclooctane–norbornene transfer-dehydrogenation catalyzed by  $[RhL_2Cl]_2$  at various concentrations of  $[RhL_2Cl]_2$ . Conditions: 50 °C; cyclooctane/benzene solution (5:3); 1600 Torr of  $H_2$ ; 1.7 M norbornene.

catalyst system			
$RhL_3Cl/H_2$	20%	30%	50%
$RhL_2Cl(CO)/hv$	20%	27%	54%
$RhL_2Cl(P^iPr_3)/H_2$	27%	11%	63%

**Figure 6.** Product distributions for isopropylcyclohexane dehydrogenation. Values were obtained by extrapolation to initial time (see Experimental Section).

major products are observed, the  $RhL_2(P^iPr_3)Cl/H_2$  thermal system affords a different distribution (Figure 6), in particular, a higher ratio of 4- to 3-isopropylcyclohexene. This may indicate participation of an intermediate such as  $RhL(P^iPr_3)Cl$ , which could be more sensitive to steric factors than  $RhL_2Cl$ .

**Summary and Conclusions.**  $RhL_2Cl$  has previously been demonstrated to dehydrogenate alkanes when generated by photodissociation of CO from  $RhL_2Cl(CO)$  (1). Under hydrogen

atmosphere, 1 is found to effect the first highly efficient, thermal, catalytic transfer-dehydrogenation of alkanes. Although photochemically inactive, other complexes containing the  $RhL_2Cl$  moiety,  $RhL_2Cl(PR_3)$  ( $R = Me, Cy, ^iPr$ ) and  $[RhL_2Cl]_2$ , are significantly more effective than 1 as thermal catalysts (like 1, only under hydrogen atmosphere). It is proposed that the role of dihydrogen is to add to the four-coordinate rhodium centers, giving octahedral dihydride complexes which then lose  $L'$ , or dissociate in the case of  $[RhL_2Cl]_2$ . (This behavior is precedented; the rate of loss of  $PPh_3$  is  $310\ s^{-1}$  for  $H_2Rh(PPh_3)_3Cl$  versus  $0.7\ s^{-1}$  for  $Rh(PPh_3)_3Cl$ .<sup>27,28</sup>) The resulting intermediate,  $H_2RhL_2Cl$ , then hydrogenates a sacrificial olefin to give the active fragment  $RhL_2Cl$ . Thus, loss of  $L'$  (or dissociation of  $[RhL_2Cl]_2$ ) is achieved by being coupled with olefin hydrogenation. We note that this approach to catalytically generating a vacant coordination site could potentially find applications in chemistry unrelated to dehydrogenation.

The fairly wide range of  $RhL_2Cl$ -based systems found to catalyze hydrogen-induced alkane transfer-dehydrogenation, and the kinetic experiments described herein, generally support the intermediacy of the  $H_2RhL_2Cl/RhL_2Cl$  couple. A detailed mechanistic picture, however, will require a thorough kinetic study, which is currently underway using the simplest of these systems, that based on  $H_2RhL_3Cl$ .

### Experimental Section

**General Procedures.** All catalytic reactions conducted under pressures greater than 3 atm (2280 Torr) were carried out in a Parr Bomb with a nominal capacity of 25 mL. Solutions (1.0–2.5 mL) were contained in a 19 mm o.d. cylindrical borosilicate glass sleeve and were magnetically stirred. (With the bomb cylinder open, it could be seen that conventional magnetic stirplate/stirbar systems functioned normally.) Solution volumes were occasionally varied in order to test if rates were limited by diffusion between solution and gas phases (since surface area remains constant, diffusion limitation should be more important with greater volumes); only for the case of 1-catalyzed reactions was the rate observed to be dependent on solution volume.<sup>20</sup> The solutions were not in contact with any metal parts. A thermocouple above the solutions was connected to a Parr Model 4842 PID temperature control system with a mantle heating system. Solutions were prepared, and the bomb was sealed under nitrogen atmosphere in a Vacuum Atmospheres glovebox; the bomb was removed, and dihydrogen was added slowly during heating. After the desired reaction time had elapsed, the bomb was placed in an ice bath to quench the reaction and opened in ambient atmosphere, and the solution was quickly sampled by GC. In some cases, the bomb was purged with CO before opening (converting  $RhL_2ClL'$  or  $[RhL_2Cl]_2$  to 1); this had no observable effect on the distribution of organic products. Solutions in the bomb were not used for catalysis after sampling.

Catalytic reactions conducted under pressures less than or equal to 3 atm were carried out in a fully anaerobic liquid-immersible cell constructed so as to hold a relatively large volume of gas over a small volume of solution in a thermostated oil bath. The cell design provided the large ballast necessary at low hydrogen pressures while permitting convenient sampling and minimizing (1) the condensation of volatile organics and (2) the difference in hydrogen pressure over solution vs hydrogen pressure in the ballast cell, which results from a difference in solvent vapor pressure if the two compartments are at different temperatures. An 18 mm i.d. "bumpy-bottom" sample cell (with stirbar) and a 50 mm i.d. cylindrical ballast are connected to the bottom side of horizontally held 7 mm i.d. tubing. A Kontes high-vacuum valve and an Ace-Thread bushing adapter are connected to the top side of the 7 mm i.d. tubing. The Ace-Thread adapter is positioned directly above the sample cell and angled 45° toward a small (ca. 0.2 mL) reservoir; for periodic sampling, the solution is tipped into the reservoir and taken into a 1.0- $\mu$ L syringe through a three-layer silicone rubber septum. Samples were loaded in the glovebox and then subjected to at least two freeze–pump–thaw cycles before the hydrogen atmosphere was added. For runs in which less than 800 Torr of  $H_2$  was added, the required amount of argon was added to bring the total pressure inside the cell to 800 Torr.

$[RhL_2Cl]_2$  was synthesized by the method of Werner.<sup>25</sup> 1 was synthesized as described previously.<sup>8,24,30</sup> The following chemicals were

(28) This result argues against the possibility that  $H_2$  addition to the rhodium center is directly promoting C–H bond addition. For examples of possible C–H addition to  $H_2$  or C–H adducts see: (a) Jobling, M.; Howdle, S.; Healy, M. A.; Poliakoff, M. *J. Chem. Soc., Chem. Commun.* **1990**, 1287–1290. (b) Bloyce, P. E.; Rest, A. J.; Whitwell, I.; Graham, W. A. G.; Holmes-Smith, R. *J. Chem. Soc., Chem. Commun.* **1988**, 846–848. (c) Hartwig, J. F.; Andersen, R. A.; Bergman, R. G. *J. Am. Chem. Soc.* **1991**, *113*, 6492–6498. (d) Jones, W. D.; Maguire, J. A. *Organometallics* **1986**, *5*, 590–591.

(29) (a) Wink, D. A.; Ford, P. C. *J. Am. Chem. Soc.* **1985**, *107*, 5566–5567. (b) Wink, D. A.; Ford, P. C. *J. Am. Chem. Soc.* **1985**, *107*, 1794–1796. (c) Wink, D. A.; Ford, P. C. *J. Am. Chem. Soc.* **1987**, *109*, 436–442.

(30) Deeming, A. J.; Shaw, B. L. *J. Chem. Soc. A* **1966**, 597.

obtained commercially: trimethylphosphine, triisopropylphosphine, tricyclohexylphosphine, tri-*p*-tolylphosphine (Strem); rhodium trichloride hydrate (Fisher); deuteriobenzene, benzene, THF, hexanes, cyclooctane, cyclooctene, norbornene, norbornane, cyclohexane, isopropylcyclohexane, 1-isopropylcyclohexene (Aldrich); 3-isopropylcyclohexene, 4-isopropylcyclohexene (Aldrich specialty chemicals). Isopropylidene-cyclohexane was prepared by the McMurry coupling of acetone and cyclohexanone.<sup>31</sup> Vinylcyclohexane was prepared by coupling  $\text{Ph}_3\text{P}=\text{CH}_2$  and  $\text{C}_6\text{C}(\text{O})\text{Me}$ .<sup>32</sup> All solvents were purified using accepted procedures<sup>33,34</sup> and removed unsaturated hydrocarbon impurities, dried over  $\text{CaCl}_2$ , and distilled from purple sodium/benzophenone ketyl solutions under argon. Hydrogen was used as supplied by Matheson, 99.999% grade except for experiments designed to determine the possible effects of impurities (99.99% grade). All other gases were used as supplied by Linde Corp. except argon, which was passed through 4-Å sieves and a manganese-oxygen scrubber. The same stock solutions and gas cylinders were used throughout each series of kinetic experiments to maximize self-consistency. Stock solutions were stored at  $-35^\circ\text{C}$  in a freezer built into the glovebox.

Gas chromatographic analyses for experiments with cycloalkanes were performed with a temperature-programmed Varian 3400 GC using a 50-m HP-1 (cross-linked) methyl silicone gum phase) capillary column with a flame ionization detector. Calibration curves were prepared using authentic samples. The identities of cyclooctene and norbornane were further confirmed by comparison with authentic samples using a Hewlett-Packard 5890A/5971A GC/quadrupole mass spectrometer. All NMR spectra were obtained on either a Varian 200- or a Varian 400-MHz instrument, using deuteriobenzene as solvent (and residual  $\text{C}_6\text{D}_6$  as reference,  $\delta$  7.15) unless otherwise noted.

**Synthesis of  $\text{RhL}_2\text{CIL}'$  Complexes.**  $\text{RhL}_2\text{Cl}$  was synthesized by the method of Wilkinson.<sup>24</sup> Low-temperature recrystallization followed addition of hexanes to a toluene solution of the crude product. Large crystals of  $\text{RhL}_2\text{Cl}$  were isolated and washed with cold hexanes. Analysis of the compound and its dihydrogen adduct was performed by  $^1\text{H}$  NMR.<sup>24</sup>

$\text{RhL}_2\text{CIL}'$  ( $\text{L}' = \text{P}^i\text{Pr}_3$ ,  $\text{PCy}_3$ ,  $\text{P}(\text{OPh})_3$ ) were prepared by slow addition of 2.0 equiv of  $\text{L}'$  to benzene solutions of  $[\text{RhL}_2\text{Cl}]_2$  (0.04 M) in the glovebox. Hexanes were then added until the cloud point was reached, and the solutions were cooled to  $-35^\circ\text{C}$  until orange-yellow crystals (except  $\text{RhL}_2\text{Cl}[\text{P}(\text{OPh})_3]$  which is yellow) formed.  $\text{RhL}_2\text{Cl}$  was characterized by its simple  $^1\text{H}$  NMR spectrum.<sup>24</sup> The  $^1\text{H}$  NMR spectrum of  $\text{Rh}(\text{PMe}_3)_2(\text{P}^i\text{Pr}_3)\text{Cl}$  indicated a mixture of *cis* and *trans* isomers, which was confirmed by the  $^{31}\text{P}$  NMR spectrum (2:1 *cis:trans*). The complex hydride region of the  $\text{H}_2$  addition products, *cis,mer*- $\text{H}_2\text{Rh}(\text{PMe}_3)_3\text{Cl}$  and *cis,trans*- $\text{H}_2\text{Rh}(\text{PMe}_3)_2(\text{P}^i\text{Pr}_3)\text{Cl}$ , matched well with computer-simulated spectra with fully reasonable  $J$  values. *cis,trans*- $\text{H}_2\text{Rh}(\text{P}^i\text{Pr}_3)_2\text{Cl}$  was identified by its reported characteristic  $^1\text{H}$  NMR spectrum.<sup>12</sup>

*trans*- $\text{Rh}(\text{PMe}_3)_2(\text{P}^i\text{Pr}_3)\text{Cl}$   $^{31}\text{P}$  NMR:  $\delta$  -0.1 (1 P, d of t,  $J_{\text{PRh}} = 179.0$ ,  $J_{\text{PP}} = 46.4$ ,  $\text{P}^i\text{Pr}_3$ );  $\delta$  -11.2 (2 P, d of d,  $J_{\text{PRh}} = 131.1$ ,  $J_{\text{PP}} = 46$ ,  $\text{PMe}_3$ ). ( $J$  values are given in hertz throughout.)

*cis*- $\text{Rh}(\text{PMe}_3)_2(\text{P}^i\text{Pr}_3)\text{Cl}$   $^{31}\text{P}$  NMR:  $\delta$  -2.8 (1 P, d of d of d,  $J_{\text{PRh}} = 183.7$ ,  $J_{\text{PP}} = 49.3$ ,  $J_{\text{PP}} = 38.6$ ,  $\text{PMe}_3$  *trans* to Cl);  $\delta$  -10.5 (1 P, d of d of d,  $J_{\text{PRh}} = 131.4$ ,  $J_{\text{PP}} = 49.3$ ,  $J_{\text{PP}} = 345.0$ ,  $\text{PMe}_3$  *trans* to  $\text{P}^i\text{Pr}_3$ );  $\delta$  45.3 (1 P, d of d of d,  $J_{\text{PRh}} = 136.4$ ,  $J_{\text{PP}^i\text{Pr}_3} = 345.0$ ,  $J_{\text{PP}^i\text{Pr}_3} = 38.7$ ,  $\text{P}^i\text{Pr}_3$ ).

*cis,trans*- $\text{H}_2\text{Rh}(\text{PMe}_3)_3\text{Cl}$   $^1\text{H}$  NMR:  $\delta$  -9.19 (1 H, d of m,  $J_{\text{HP}^i\text{Pr}_3} = 178.6$ ,  $J_{\text{HP}^i\text{Pr}_3} = 15.6$ ,  $J_{\text{HRh}} = 12.3$ ,  $J_{\text{HH}} = 7.5$ , RhH *trans* to  $\text{PMe}_3$ );  $\delta$  -18.60 (1 H, m (14 peaks),  $J_{\text{HP}^i\text{Pr}_3} = 19.0$ ,  $J_{\text{HP}^i\text{Pr}_3} = 23.7$ ,  $J_{\text{HRh}} = 11.4$ ,  $J_{\text{HH}} = 7.5$ , RhH *trans* to Cl);  $\delta$  1.32 (18 H, partly resolved virtual triplet, ( $^2J_{\text{PH}} + ^4J_{\text{PH}})/2 \sim 3.3$ , *trans*  $\text{P}(\text{CH}_3)_3$  ligands);  $\delta$  1.11 (9 H, d,  $^2J_{\text{PH}} = 6.7$ ,  $\text{P}(\text{CH}_3)_3$  *trans* to hydride).

*cis,trans*- $\text{H}_2\text{Rh}(\text{PMe}_3)_2(\text{P}^i\text{Pr}_3)\text{Cl}$ :  $\delta$  -10.25 (1 H, d of m,  $J_{\text{HP}^i\text{Pr}_3} = 172.1$ ,  $J_{\text{HP}^i\text{Pr}_3} = 16.5$ ,  $J_{\text{HRh}} = 12.1$ ,  $J_{\text{HH}} = 8.2$ , RhH *trans* to  $\text{P}^i\text{Pr}_3$ );  $\delta$  -19.60 (1 H, m (14 peaks),  $J_{\text{HP}^i\text{Pr}_3} = 13.3$ ,  $J_{\text{HP}^i\text{Pr}_3} = 19.1$ ,  $J_{\text{HRh}} = 13.3$ ,  $J_{\text{HH}} = 8.2$ , RhH *trans* to Cl).

**Experiments with  $\text{RhL}_2\text{CIL}'$ .** The general procedure was as described above. In a preliminary set of runs at  $60^\circ\text{C}$  with 1.7 M norbornene and 1.0 mM  $\text{RhL}_2\text{CIL}'$  ( $\text{L}' = \text{P}^i\text{Pr}_3$ ,  $\text{PCy}_3$ ) under 800 Torr of  $\text{H}_2$ , the rates of cyclooctene formation were found to be 0.79 and 0.61 mM/min, respectively, while the respective rates of norbornane formation was 4.5 and 6.8 mM/min. Since the ratio of cyclooctene:norbornane formation was greater for the  $\text{P}^i\text{Pr}_3$  complex, it was chosen for further experiments, specifically determination of the  $\text{H}_2$  pressure dependence.

To 0.8 mL of a stock cyclooctane solution of  $\text{Rh}(\text{PMe}_3)_2\text{Cl}(\text{P}^i\text{Pr}_3)$  (0.6 mM) was added norbornene (0.16 g; 1.7 mmol), bringing the total vol-

ume to 1.0 mL and the concentrations of norbornene and  $\text{Rh}(\text{PMe}_3)_2\text{Cl}(\text{P}^i\text{Pr}_3)$  to 1.7 M and 0.48 mM, respectively. At  $50^\circ\text{C}$ , individual bomb runs were conducted for 30 and 60 min; ballast cell runs were each sampled at 30 and 60 min. Product formation was found to be linear with time.

**NMR Characterization of  $[\text{RhL}_2\text{Cl}]_2$  Reaction Solutions.** In a typical experiment,  $[\text{RhL}_2\text{Cl}]_2$  (5 mM) in  $\text{C}_6\text{D}_6$  containing cyclohexene (0.021 M) was freeze-pump-thawed and placed under dihydrogen atmosphere (1600 Torr).  $^1\text{H}$  NMR of the solution, immediately after thawing and shaking, showed hydride resonances assignable to two complexes. In analogy with  $\text{H}_2\text{RhL}'_2(\mu\text{-Cl})_2\text{RhL}'_2$  ( $\text{L}' = \text{P}(p\text{-C}_6\text{H}_4\text{Me})_3$ ),<sup>26</sup> one resonance is attributed to the equivalent terminal hydrides of  $\text{H}_2\text{RhL}'_2(\mu\text{-Cl})_2\text{RhL}'_2$ :  $\delta$  -20.52, d of t,  $J_{\text{RH}} = 29.1$ ,  $J_{\text{PH}} = 19.7$ . The second complex, believed to be an isomer of  $\text{H}_2\text{RhL}'_2(\mu\text{-Cl})_2\text{RhL}'_2$ , exhibits two resonances, including one assigned to a terminal hydride ( $\delta$  -17.69, d of t of d,  $J = 17.1$ , 17.0, 3.7). A highly complex multiplet at  $\delta$  -19.86 (ca. 30 resolvable peaks, with separations of 3.7 Hz attributed to coupling with the terminal hydride) is attributed to a bridging hydride of the same complex. The integrals of the two resonances assigned to the second complex ( $\delta$  -17.69 and -19.86) remained equal within 5% throughout numerous experiments, in both the presence and the absence of olefin, and throughout the decomposition process noted below. The ratio of total hydride resonance integrals of the all-terminal and bridging/terminal complexes remained constant at 1:3. The  $\text{PMe}_3$  methyl proton region of the spectrum is complicated by the cyclohexene protons as well as overlapping protons of the several inequivalent phosphines, but the ratio of  $\text{PMe}_3$  to hydride resonance integrals remained constant at 18:1 ( $\pm 20\%$ ) in the presence of olefins. In the absence of added olefin, the same two species are initially observed but rapidly ( $<15$  min) disappear. New resonances associated with several (uncharacterized) species appear as the initial hydrides decompose. We were unable to obtain useful  $^{31}\text{P}$  NMR data, partly because the time required to collect data was too great compared with the times of decomposition in the absence of olefin and consumption of dissolved hydrogen in the presence of olefin.

**Kinetic Experiments with  $[\text{RhL}_2\text{Cl}]_2$ .** The general procedure was as described above. Turnover numbers refer to mole of product per mole of  $[\text{RhL}_2\text{Cl}]_2$  (not per mole rhodium). In all cases, product formation was found to be linear with time.

For the hydrogen-dependence experiments a 4:1 (v:v) cyclooctane:benzene solvent system was used. Norbornene (0.48 g; 5.1 mmol) was added to 2.4 mL of a 0.6 mM solution of  $[\text{RhL}_2\text{Cl}]_2$ , bringing the total volume to 3.0 mL and the concentrations of norbornene and  $[\text{RhL}_2\text{Cl}]_2$  to 1.7 M and 0.48 mM, respectively. Sample volumes were 1.0 mL. Runs were carried out in both the bomb and ballast cell at 2280 Torr (3 atm). The bomb values were consistently higher by a factor of 1.10 (probably due to a small temperature difference between the bomb and ballast cell, both nominally at  $50^\circ\text{C}$ ). Turnover numbers for all bomb runs (i.e., pressures greater than 3.0 atm) in this series were therefore multiplied by 0.91 for self-consistency. Bomb runs were conducted for 30 and 60 min. Ballast cell runs were sampled at 30, 60, and 90 min.

For the  $[\text{RhL}_2\text{Cl}]_2$  concentration-dependence experiments a 4:3:2 cyclooctane:benzene:norbornene solvent system was used (the greater fraction of benzene was necessary to dissolve greater concentrations of  $[\text{RhL}_2\text{Cl}]_2$ ). The sample volume was 1.0 mL. All samples were prepared by dilution of a 4.0 mM stock solution to give the desired concentration of  $[\text{RhL}_2\text{Cl}]_2$ . Reactions were conducted in the ballast cell at  $50^\circ\text{C}$  under 1600 Torr of dihydrogen and monitored every 10–15 min for an interval of 60 min.

For the norbornene concentration-dependence experiments, a 3.7 M concentration of cyclooctane was maintained (50% by volume); [norbornene] was varied from 0.17 M (2.0%) to 1.7 M (20%), while the remainder of the solvent system was benzene. The sample volume was 1.0 mL. Reactions were conducted in the ballast cell at  $50^\circ\text{C}$  under 1600 Torr of dihydrogen and monitored every 10–15 min for a total of 60 min.

**Isopropylcyclohexane Dehydrogenation.** An isopropylcyclohexane solution of  $\text{RhL}_2\text{Cl}(\text{P}^i\text{Pr}_3)$  (1.0 mM) and norbornene (1.7 M) under 800 Torr of  $\text{H}_2$  was maintained at  $60^\circ\text{C}$  and sampled periodically. The reported ratios are numbers obtained by extrapolation back to zero time of the plot of isotopic ratios vs time. The initially measured (45 min) distribution was 27.1, 11.4, 61.5 for vinylcyclohexane, 3-isopropylcyclohexene, 4-isopropylcyclohexene; cf. the respective extrapolated values of 26.5, 10.6, 62.9. A similar procedure was used for  $\text{RhL}_2\text{Cl}$ , although a longer time was required to obtain reliably measurable levels of alkene and the change of the distribution (due to isomerization or rehydrogenation) with time was relatively more severe. The initially measured (120 min) distribution was 20, 20, 61 for vinylcyclohexane, 3-isopropylcyclohexene, 4-isopropylcyclohexene vs respective extrapolated values of 20, 30, 50. The respective values for 1-photocatalyzed dehydrogenation (in neat isopropylcyclohexene (conducted as described previously)<sup>8</sup> were

(31) McMurry, J. E. *Acc. Chem. Res.* 1983, 16, 405–411.

(32) Rubottom, G. M.; Kim, C. *J. Org. Chem.* 1983, 48, 1550–1552.

(33) Gordon, A. J.; Ford, R. A. *The Chemist's Companion*; Wiley Interscience: New York, 1972; pp 429–437.

(34) Perrin, D. D.; Armarego, W. L. F.; Perrin, D. R. *Purification of Laboratory Chemicals*; Pergamon Press: Oxford, U.K., 1980; 118–119.

initially (120 min) 20.5, 26.7, 52.8, and the extrapolated values were 19.8, 26.6, 53.6.

The isopropylcyclohexene isomers were identified by comparison of their GC retention times with those of authentic samples, using a 2-m silver nitrate/tetraethylene glycol packed column made according to the procedure of Cope et al.<sup>35</sup> The assignments had previously been confirmed by using the HP-1 capillary column and dibrominating the olefins by the method of Crabtree et al.<sup>36</sup> and by comparing GC retention times

with those of the dibromides of the authentic olefins.

**Acknowledgment.** We thank the Division of Chemical Sciences, Office of Basic Energy Sciences, Office of Energy Research, U.S. Department of Energy, for support of this work. A.S.G. thanks the Camille and Henry Dreyfus Foundation for a Distinguished New Faculty Grant.

(35) Cope, A. C.; Ambros, D.; Ciganek, C. F.; Howell, C. F.; Jacura, Z. *J. Am. Chem. Soc.* **1960**, *82*, 1750-1753.

(36) Burk, M. J.; Crabtree, R. H.; McGrath, D. V. *Anal. Chem.* **1986**, *58*, 977-978.

(37) Runs involving H<sub>2</sub> pressures >3 atm were conducted in a Parr thermostated bomb; all other runs were conducted in a Pyrex vessel with a ballast completely immersed in a thermostated oil bath. The bomb gave consistently higher rates at 3 atm than the glass vessel (ca. 10%), which may be due to problems with the bomb thermostat. To compensate, all bomb data are multiplied by a constant factor (0.91).

## Mechanisms of Viologen-Mediated Charge Separation across Bilayer Membranes Deduced from Mediator Permeabilities

Sergei V. Lymar<sup>†</sup> and James K. Hurst<sup>\*</sup>

Contribution from the Department of Chemical and Biological Sciences, Oregon Graduate Institute of Science and Technology, Beaverton, Oregon 97006-1999, and Institute of Catalysis, Novosibirsk 630090, Russia. Received January 14, 1992.

Revised Manuscript Received August 21, 1992

**Abstract:** The mobilities of several bipyridinium ions across the hydrocarbon bilayer membranes of dihexadecyl phosphate (DHP) small unilamellar vesicles have been determined by measuring the uptake of <sup>14</sup>C-radiolabeled analogs. The *N*-alkyl-*N'*-methyl-4,4'-bipyridinium (viologen, C<sub>*n*</sub>MV<sup>2+</sup>) dication and the *N*-methyl-4,4'-bipyridinium cation were membrane-impermeable. However, the C<sub>*n*</sub>MV<sup>•+</sup> radical cations were permeable, provided that the *n*-alkyl chain length did not exceed 12 carbon atoms. Diffusion rates obeyed a simple first-order rate law; rate constants for *n* = 1 and *n* = 6 were nearly identical, and the constant for *n* = 12 was about 3-fold lower. From these values and the measured diffusion potential, the permeability coefficient of the *N,N'*-dimethyl-4,4'-bipyridinium radical cation was estimated to be 2 × 10<sup>-8</sup> cm s<sup>-1</sup> at 23 °C. When *n* = 16, radiolabel exchange was biphasic, with the major fraction of DHP-bound C<sub>16</sub>MV<sup>•+</sup> undergoing no transmembrane diffusion. This behavior confirms earlier suggestions, based upon the dynamics of viologen-mediated transmembrane redox reactions, that the short-chain viologens act as mobile charge relays, whereas the long-chain congeners transfer charge primarily by electron tunneling.

### Introduction

Oxidation-reduction reactions have been shown to occur across bilayer membranes in numerous asymmetrically organized redox systems.<sup>1</sup> These reactions are of considerable topical interest in relation to applications in photoconversion, "molecular" electronics, and biomimicry.<sup>1,2</sup> In every case reported, either the reactants themselves were membrane-bound or the membrane contained additional redox components capable of mediating the overall reaction. The requirement for membrane-localized redox components is consistent with the general nature of electron transfer processes, since the bilayer membrane presents an insulating barrier of 40-50-Å thickness, a distance which is too large to allow electron tunneling at appreciable rates between reactants confined to the aqueous compartments.<sup>3</sup> The molecular details of these reactions are not well characterized, however. Two alternative limiting pathways are<sup>1a</sup> (i) that membrane-bound reactants which are transversely juxtaposed in the opposite bilayer leaflets undergo electron exchange or (ii) that they diffuse across the bilayer, thereby acting as mobile redox carriers. Only in pathway i does transmembrane electron transfer actually occur.

The measurement of redox rates alone does not provide a basis for distinguishing between the limiting pathways.<sup>1a</sup> Comparison of the redox rates with independently measured rates of transmembrane diffusion of the reaction components could, in principle, resolve this issue. For example, if diffusion by all available

pathways were much slower than the overall transmembrane oxidation-reduction rate, then the reaction would involve electron transfer; in contrast, if one or more redox components were to diffuse on the same timescale as the net transmembrane redox rate, then reaction by a diffusional pathway would be plausible.<sup>1a</sup> Quantitative information on transmembrane diffusion of the reaction components has generally been unavailable, however.

We have sought to identify transmembrane redox pathways in simple vesicular systems for which the requisite diagnostic rate information can be obtained. Specifically, we have utilized anionic dihexadecyl phosphate (DHP) vesicles, which strongly bind cationic *N*-alkyl-*N'*-methyl-4,4'-bipyridinium ions (C<sub>*n*</sub>MV<sup>2+</sup>, with *n* = 1-16). We have shown that addition of membrane-impermeable strong reductants to the external medium caused one-electron reduction of internal viologens to their corresponding radical cations (C<sub>*n*</sub>MV<sup>•+</sup>) by processes mediated by the externally bound viologens.<sup>1a,4,5</sup> As with all charge separation processes

(1) For recent reviews, see: (a) Hurst, J. K. *Kinetics and Catalysis in Microheterogeneous Systems*; Surfactant Science Series, Vol. 38; Marcel Dekker: New York, 1991; pp 183-226. (b) Lymar, S. V.; Parmon, V. N.; Zamaraev, K. I. *Photoinduced Electron Transfer III*; Topics in Current Chemistry, Vol. 159; Springer-Verlag: Berlin, 1991; pp 1-66. (c) Robinson, J. N.; Cole-Hamilton, D. J. *Chem. Soc. Rev.* **1991**, *20*, 49-94.

(2) See, e.g.: (a) Grätzel, M. *Heterogeneous Photochemical Electron Transfer*; CRC Press: Boca Raton, FL, 1989. (b) Lehn, J. M. *Angew. Chem., Int. Ed. Engl.* **1990**, *29*, 1304-1319. (c) Yamazaki, I.; Tamai, N.; Yamazaki, T. *J. Phys. Chem.* **1990**, *94*, 516-525.

(3) See, e.g.: Marcus, R. A.; Sutin, N. *Biochim. Biophys. Acta* **1985**, *811*, 265-322.

\* Address correspondence to this author at Oregon Graduate Institute.

<sup>†</sup> Institute of Catalysis (visiting scientist at Oregon Graduate Institute).